FEASIBILITY OF THE DEFORMATION ANALYSIS OF A PLATE SUBJECTED TO VIBRATIONS USING RECENT COMPUTER VISION METHODS

E. Simonetto [a, *], C. Pezerat [b]

[a] L2G, ESGT, JE 2508, 1 Bd Pythagore, Campus universitaire, 72000 LE MANS, France – elisabeth.simonetto@esgt.cnam.fr
[b] LAUM, Université du Maine, CNRS UMR 6613, av. O.Messiaen, 72085 LE MANS Cedex 9, France – charles.pezerat@univ-lemans.fr

Commission III, WG III/1

KEY WORDS: computer vision, three-dimensional, dynamic model

ABSTRACT:

In this work, we deal with the measurement of dynamic displacements of a plate using modern photogrammetric techniques. This plate is subjected to vibrations whose frequencies can vary between 20 Hz and about 4000 Hz. Such analysis is particularly useful for studying excitations due to turbulent flows, which necessitates synchronous acquisitions of the displacement field. For that purpose, we propose a study of the feasibility of such measurements using a simple experimental scheme: two cameras and computer vision methods. The system sensitivity must be sub-millimetric in the plate normal direction. This study is realised by simulating the deformation pattern on a virtual plate and the acquired images. The performances of the simulated protocol is assessed in the case where the external parameters are know or unknown. In this last case, we use the five-point approach described in (Stewénius, 2006) and based on the Gröbner bases. The results show that this experimental scheme should allow sub-millimetric measurements.

1. INTRODUCTION

1.1 Purpose of this work

In the vibration and vibroacoustic domains, engineers and researchers are often interested in measuring vibration fields of mechanical structures. This is the case when they seek to study the dynamic behaviour of structures (Ewins, 2000) or to identify the vibration sources exciting the structure (Pezerat, 2000). In general, the experimental setup consists in measuring normal displacements because they are the components responsible for the radiated noise. Several experimental systems are used. The most common sensor is the piezoelectric accelerometer, which generates a signal proportional to the normal acceleration at the point where the sensor is glued. The principal disadvantage of this sensor is that it is intrusive, because its mass can change the vibration behaviour of the structure. Also, for a complete displacement field measurement, the accelerometer must be moved, restricting the study to stationary vibrations along the duration of the measurement, The other common technic is the use of a laser vibrometer giving, by optic Doppler effect, the vibration velocity of a reflective structure. Today, scanning laser vibrometers are more convenient systems allowing the facility to measure a complete vibration field of a structure without contact. Here also, the fact that point to point measurements are done, this system must be used on structure excited by a stationary source. Another way is the use of the acoustic holography. The principle consists in measuring the acoustic radiation of the structure in a plane and to compute a back propagation of this plane to the surface of the structure. A recent study on an unstationary acoustic holography was done (Thomas, 2008), but its use is still in development and necessitates a lot of microphones and an analyzer with numerous parallel tracks.

The motivation of this work is the development of an experimental technique allowing a synchronous assessment of instantaneous displacements at several points of a structure. This is the only possible way, when one wants to analyze vibrations due to unstationary sources or spatially uncorrelated sources, like the excitations by turbulent flow along the surface of a structure (Chevillotte, 2010). Thanks to the improvement of high-speed cameras, the use of computer vision methods is maybe a new original possibility with benefits non-existant in conventional vibration measurement techniques.

1.2 Methodology

This study is realised by simulating the deformation pattern on a virtual plate and the acquired images. The internal parameters of the camera are expected to be known. To process the images, the plate is covered with a regular grid clearly visible on images. Then two cases are studied where external parameters are known or not known. In the first case, tie points are matched along their epipolar lines using the fundamental matrix (Longuet-Higgins, 1981). 3-D measurements are written in the local reference system where the external parameters are provided. Studying this first case allows us to check for suitable experimental configurations and the matching processing. In the second case, bundle adjustement is classically used from coarse external parameters and known targets. However we are interested in a light equipment and simple experimental protocol, so, without prior known targets nor coarse external parameters, expect the base between the cameras. Thus, we propose to resolve the fundamental matrix using the approach described in (Stewénius, 2006) and based on the Gröbner bases. In the following of this paper, the methodology is presented in part 2. Then results are discussed in part 3.

* Corresponding author.

2. IMAGE SIMULATION AND PROCESSING

2.1 Hardware

For our purpose, we need two synchronous high-speed cameras that allow the visualization of the whole plate in the overlap between both images, a sub-millimetric precision in the plate normal direction, and insure that the grid clearly appears in both images. However, high-speed cameras have limited size of detector array, which prevents us from analysing the performances of simulated protocols according to different real camera characteristics. However, they led us to the following realistic choices:

- A camera such as the PCO.dimax: 2016x2016 pixels at 11µm, >1200 fps.
- A lens of 8mm.
- A normal configuration where the camera baseline is set to 20cm and the camera-plate distance to 15cm, which insures an overlap of 50% and a visible grid.

In this framework, the expected sensitivity in the plate normal direction is around 0.1mm.

2.2 Modelling of the plate before and during excitation

We define a plate whose size is 20cmx20cm. The spatial spacing of the points that modelize the plate (i.e. the resolution of the model) is set to 0.1mm. A regular grid covers this plate. Its thickness is set to 0.2mm and the point spacing is 0.5cm. The points on the grid are white and the other ones on the plate are medium gray. Here, an instantaneous shape is considered by a local variation of the point coordinate along the normal axis to the plate, using a cosine function (figure 1).

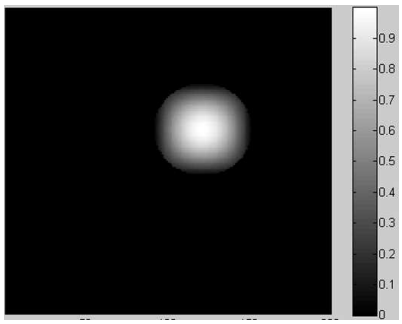

Figure 1: Instantaneous shape in the normal direction of the plate. Amplitudes vary from 0 to 1mm.

2.3 Image simulation

The images of the plate are easily obtained using the classical pine-hole camera model (figure 2). In this model, the image point is linked to the object point using the collinearity equations. In these equations, camera internal parameters (principal point offsets, optical distortion and principal distance) are also included. Besides, the camera external parameters (rotation angles of the image plane and position of the perspective center) are fixed. We introduce a viewing angle error of a few degrees (but less than 3 degrees) from the normal case. A σ-gaussian noise is also added to the image.

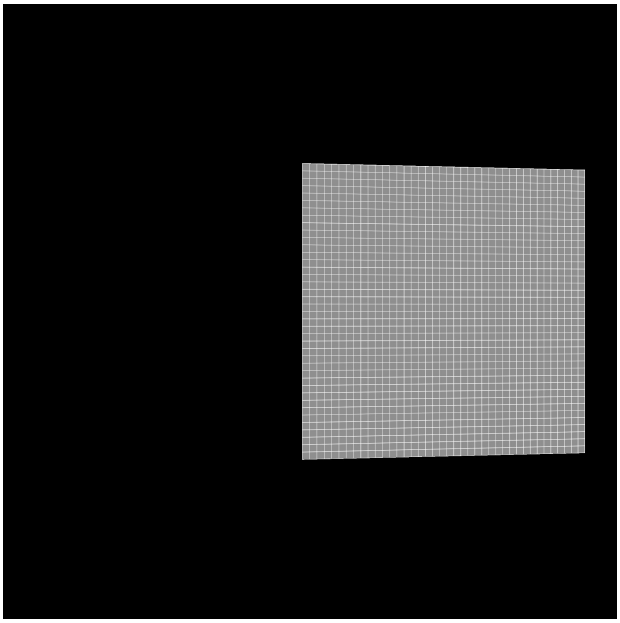

Figure 2: Simulated left image of the gray plate, covered by a white grid. Black points are not located on the plate.

2.4 Processing

We realize the following steps:

- the detection of the grid nodes on each image,
- the matching of the grid nodes between two images acquired at the same time,
- the 3-D position computation of each node and at each date,
- the temporal displacement assessment at each node.

Let us now detail these steps.

The grid nodes are the centers of white crosses. They are coarsly detected using the Harris detector (Harris, 1988) then a refinement stage leads to a precise sub-pixellic position. It consists in adjusting the node location using a correlation processing with the ideal cross (figure 3). This approach enables to take into account the grid image deformation due to the perspective viewing and the plate excitation. Almost all nodes are detected (figure 4).

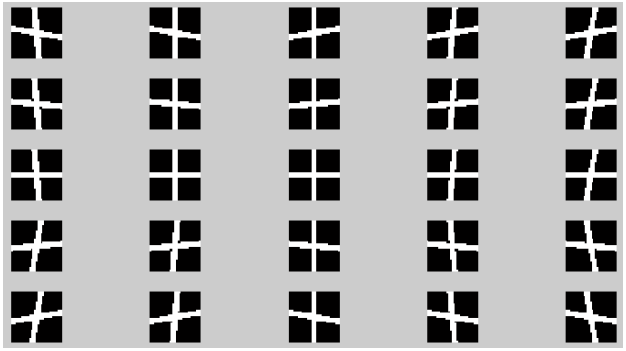

Figure 3: Example of 25 models of cross used to fit the location of the grid nodes.

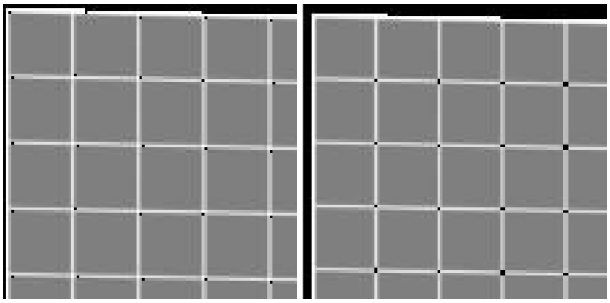

Figure 4: Image subarea displaying the detected Harris corner in black (at left) and the refined node location (at right). The node is located at the center of the displayed black feature with a precision of half a pixel.

Once the nodes are detected on all images, the stereo-matching is performed between two stereoscopic views acquired at the same time. This step uses the epipolar directions computed from the essential matrix (Longuet-Higgins, 1981). If the internal and external parameters are known, the homologous nodes are easily found. Their 3-D location is then derived from collinearity equations. They are provided in the reference system of the scene.

In the case of unknown external parameters, we propose to solve the relative orientation in four steps:

(1) *The automatic matching of the grid nodes*. This is possible because almost all nodes are detected and constitute a regular grid, although the plate deformation. Indeed, the deformation of the plate is very weak, as a consequence, the displacement of the grid nodes in the images is only of some pixels. Then, the regular spacing between two consecutive nodes in the image is assessed with a good precision. Detected nodes are sorted column by column. For each column, since the expected number of nodes is known, we address a 1 if the node is detected and a 0 otherwise. Two stereoscopic columns are then associated leading to the pairs of homologuous nodes.

(2) *The computation of the possible essential matrices*. From these pairs, the essential matrix can be computed. We are confronted to the 3-D reconstruction of a quasi-planar surface. For that reason, we use the five-point approach described in (Stewénius, 2006) and freely available[1]. In this approach, the essential matrix is described in the four-dimensional null-space with three unknowns:

$$E = xE_1 + yE_2 + zE_3 + E_4 \quad (1)$$

where E = essential matrix
E_1, E_2, E_3, E_4 = four null-space basis vectors
x, y, z = three unkowns to determine

The null-space basis is derived from the epipolar constraints of each pair of homologuous points, where E is described by nine unknowns:

$$x_2^T A_2^{-T} E A_1^{-1} x_1 = 0 \quad (2)$$

where x_1, x_2 = two homologuous points in the left and right images respectively

[1] http://vis.uky.edu/~stewe/FIVEPOINT (accessed May 2010)

A_1, A_2 = left and rigth intrinsec matrices

These equations are written as a linear system:

$$MX = 0 \quad (3)$$

where X = vector that contains the nine terms of E

The four null-space vectors are the four singular vectors corresponding to the four smallest singular values of M.
Then the three unknowns, x, y and z, are computed from the ten following equations:

$$\begin{cases} \det(E) = 0 \\ 2EE^T E - trace(EE^T)E = 0 \end{cases} \quad (4)$$

In (Stewénius, 2006), a polynomial resolution is proposed. It is based on the recognition of a Gröbner basis that is defined by ten monomials in x, y and z. This leads to ten solutions. Among these solutions, we retain the real ones.

(3) *The choice of the essential matrix*. For each possible essential matrix, E, we compute the 3-D points in the scene using equations 6 and 7. The retained essential matrix is the one that maximises the depth of the points. In order to obtain the 3-D points from equations 6 and 7, the essential matrix is described by rotation and translation (Longuet-Higgins, 1981):

$$E = [T]_X R \quad (5)$$

where R, T = rotation matrix and translation vector
$[.]_X$ = skew-symmetric matrix operator

R and T are estimated from the Singular Value Decomposition (SVD) of E. The image point is linked to its scene point by:

$$\begin{cases} M = \lambda_1 A_1^{-1} x_1 \\ M = \lambda_2 R^T A_2^{-1} x_2 - \gamma R^T T \end{cases} \quad (6)$$

where M = scene point
λ_1, λ_2 = left and right point depths
γ = scale factor

The depths are deduced by resolution of the following linear system (including all pairs of point) using SVD (see for example Ma, 2006):

$$\lambda_1 [A_2^{-1} x_2]_X R A_1^{-1} x_1 + \gamma [A_2^{-1} x_2]_X T = 0 \quad (7)$$

For each E, two solutions for R and T exist, leading to four possible projection models. However, only one is expected to produce scene points with positive left and right depths.

At the end of this step, we obtain the scene points in the reference system of the left camera. Besides the cloud of 3-D points is given up to an universal scale.

(4) *The computation of the 3-D points for each acquisition time at the same scale*. We assume that the distance between the two cameras can be known quite precisely. Thus, the translation T related to the essential matrix is modified in order to produce the 3-D points at the correct scale.

To access to the temporal 3-D displacement, the grid nodes are tracked in consecutive views acquired by the same camera. As the displacement in the image is very small, it only consists in associating one node to the nearest one in the previous image. This step also enables to delete false node detection as a node must be detected in all images.

Finally we produce two interpolated displacement maps. The first one is related to the displacement in the plane of the plate, that is the planimetric displacement map. The second one corresponds to the displacement in the normal direction of the plate, denoted the normal displacement map.

3. RESULTS ANALYSIS

3.1 Known external parameters

First, we verify the precision of the 3-D retrieval when the external parameters are known. Figure 5 shows the normal displacement error map compared to the true map. Before any deformation of the plate, the figure presents:

$$N_{before} - N_{true,before} \quad (8)$$

where N_{before} = estimated map before any deformation
$N_{true,before}$ = true map before any deformation

After the deformation, the figure shows:

$$(N_{after} - N_{before}) - (N_{true,after} - N_{true,before}) \quad (9)$$

where N_{after} = estimated map after the deformation
$N_{true,after}$ = true map after deformation (see figure 1)

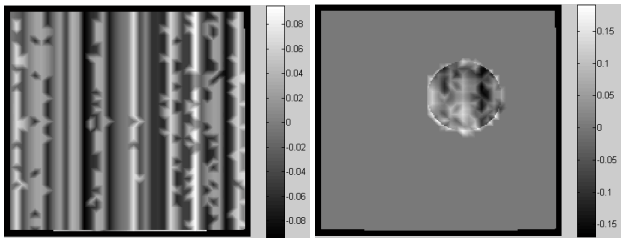

Figure 5: Interpolated map of the error of the normal displacements (in mm) when the external parameters are known: (Left) before the deformation of the plate. (Right) after the deformation.

It turns out that our 3-D reconstruction algorithm based on the collinearity equations leads to residual errors of around 0.1mm in the normal direction. This is consistent with the expected accuracy of the equipment configuration. The deformation shape is well recognized and some errors could probably be reduced by a low-pass filtering.

3.2 Unknown external parameters

When the external parameters are unknown, the relative orientation resolution leads to a good estimation of the essential matrix. Indeed, if we compare the rotation and translation obtained from this essential matrix and then from the true one, we find that the rotation matrices are identical and the translation differs, despite the scale factor, in the Z-component of around 0.04%.

The obtained 3-D points are expressed in the left camera reference system. In order to evaluate the reconstruction accuracy, the model should be oriented in the scene reference system. However, as we are only interested in the relative motion of the plate and in order to be free from defining scene targets prior the measurements, we make the comparison in the left camera reference system. For that purpose, we compute the displacements in the left camera reference system using the estimated essential matrix on the one hand and the true essential matrix on the other hand and compare them. Figure 7 displays the obtained 3-D points from the estimated essential matrix. Figure 8 shows the displacement errors in the Z direction before and after the deformation. Like previously (equation 9), the displacement error measured after the deformation takes into account the estimated state of the plate before any deformation. We observe that the external parameter estimation is accurate and do not induce significant additional errors (only some microns).

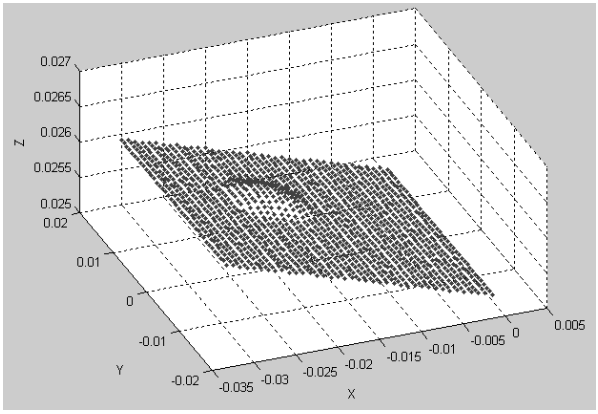

Figure 7: 3-D points from the estimated essential matrix.

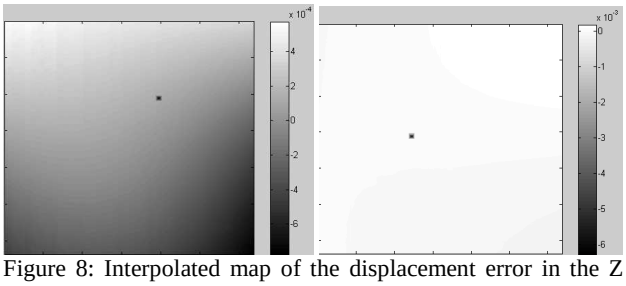

Figure 8: Interpolated map of the displacement error in the Z direction (in mm) when the external parameters are unknown: (Left) before the deformation of the plate. (Right) after the deformation.

4. CONCLUSION

The results shown in this paper are obtained from ideas coming from different scientific domains. At the moment, validations are only numerical, but obtained precision allows thinking the possibility to measure vibration displacements. In the future, interests will be focused on the establishment of algorithms to process video images on complete simulations. Then, real experimentations could be investigated on a plate excited by a stationary source, where comparisons with scanning laser vibrometer and acoustic holography technics should give interesting references. Finally, the ultimate goal is to test this original technic for non-stationary vibrations which constitutes the most advantage of this approach.

5. REFERENCES

Chevillotte, F., Leclere, Q., Totaro, N., Pezerat, C., Souchotte, P., Robert, G., 2010. Identification d'un champ de pression pariétale induit par un écoulement turbulent à partir de mesures vibratoires (Identification of the parietal pressure field induced by a turbulent flow from vibration measurements). In : *Congrès Français d'Acoustique*, Lyon, France, http://cfa.sfa.asso.fr/cd1/data/articles/000271.pdf

Ewins, D.J., 2000. *Modal Testing: Theory, Practice and Application*. Hertfordshire: Research Studies Press.

Harris, C., Stephens, M., 1988. A combined corner and edge detector. *Proc. 4th Alvey Vision Conference*, pp. 147-151.

Longuet-Higgins, H., 1981. A computer algorithm for reconstructing a scene from two projections. *Nature*, 293 (10), pp. 133-135.

Ma, Y., Soatto, S., Kosecka, J., Shankar Sastry, S., 2006. *An invitation on to 3-D Vision*. Springer.

Pezerat, C., Guyader, J.L., 2000. Force Analysis Technique: Reconstruction of Force Distribution on Plates. *Acustica united with Acta Acustica*, 86, pp. 322-332.

Stewenius, H., Engels, C., Nister, D., 2006. Recent Developments on direct relative orientation. *ISPRS Journal of Photogrammetry and Remote Sensing*, 60, pp. 284–294.

Thomas, J.-H., , Grulier, V., Paillasseur, S., Pascal, J.-C., 2008. Real-time nearfield acoustic holography : implementation of the direct and inverse impulse responses in the time-wavenumber domain. In: *Proceeding of ICSV15*, Daejeon, Korea.